EUROPEAN FUSION DEVELOPMENT AGREEMENT

EFDA–JET–PR(04)06

S.K. Erents, R.A. Pitts, W. Fundamenski, J.P. Gunn, G.F. Matthews
and JET EFDA contributors

A Comparison of Experimental Measurements and Code Results to Determine Flows in the JET SOL

A Comparison of Experimental Measurements and Code Results to Determine Flows in the JET SOL

S.K. Erents[1], R.A. Pitts[2] , W. Fundamenski[1], J.P. Gunn[3] and G.F. Matthews[1]
and JET EFDA contributors*

[1]EURATOM/UKAEA Fusion Association, Culham Science Centre, Abingdon, OX14 3DB, UK
[2]Centre de Recherches en Physique des Plasmas, Association EURATOM – Confédération Suisse cole Polytechnique Fédérale de Lausanne, CH-1015 Lausanne, Switzerland.
[3]Association CEA-EURATOM sur la fusion controlee, 13108 Saint Paul Lez Durance, France.
** See annex of J. Pamela et al, "Overview of Recent JET Results and Future Perspectives", Fusion Energy 2000 (Proc. 18th Int. Conf. Sorrento, 2000), IAEA, Vienna (2001).*

Preprint of Paper to be submitted for publication in
Plasma Physics and Controlled Fusion

ABSTRACT.

Two reciprocating probe systems, in the same poloidal position at the top of the JET torus but toroidally separated by 180^{o}, have been used to measure parallel flow in the Scrape-Off Layer (SOL). One system uses the entrance slit plates of a Retarding Field Analyser (RFA) to record upstream and downstream flux densities, and the second system uses two pins of a nine pin Turbulent Transport Probe, (TTP). Measurements have been made in both forward and reverse field directions. Results from both systems are similar.

In the forward field direction, that is with $\vec{\nabla B}$ drifts downward towards the divertor, there is a strong parallel flow in the direction outer to inner divertor. The flow generally has a low value, Mach number M~0.2, close to the separatrix and rises in the region of high magnetic shear close to the separatrix to a maximum of M~0.5 some 20mm outside of the separatrix. The flow in the reverse field direction is small, close to zero, and generally is again in the same direction as that for forward field close to the separatrix, with M~0.2. Code results using EDGE2D with drifts suggested an almost symmetrical flow about zero when the field direction was changed in an earlier work, [1]. However, this was for particularly low density, high temperature edge conditions, and the predicted symmetry is not evident for more usual edge conditions, reported here. Experimentally, the flow is found to be quite asymmetric about zero, particularly at high density. There is some symmetry in flow, but about an offset value of M~0.2. The form of M(r) is similar to experiment but the major code result is the low value of M generally < 0.1. The effect of gas (deuterium) and impurity (carbon) puffing in the code has been investigated. We are unable to say why the magnitude of M(r) from experimental data and codes do not agree. However, results presented in this paper suggest that the probe itself may be exhibiting an influence on the magnitude of the flow as measured in the SOL.

1. INTRODUCTION

Measurements of a strong parallel flow of plasma ions with Mach numbers ~0.5, in the direction from outer to inner divertor in JET, were reported in [1]. This flow was suggested as a possible cause of the large build up of carbon (and trapped tritium) at the inner divertor louvers by frictional coupling between the hydrogenic ions and the carbon impurities sputtered from the outer divertor target plates, [2]. Other investigations using a Turbulent Transport Probe (TTP) in the Scrape-Off Layer (SOL) have shown that there is experimental evidence for a dynamic coupling between turbulent transport and parallel flows, suggesting the 'extra' mechanism responsible for the high Mach numbers measured in the SOL are closely linked with turbulent transport events, [3]. Other evidence that the strong flow really exists, i.e. is not just due to false interpretation of the flux measurements on each side of the probes, comes from ion temperature, Ti(r), measurements on each side of the probes, [4]. These are indeed different – a situation which has been predicted to occur in the presence of strong flow, [5].

LaBombard, [6], found that in Alcator C-Mod the poloidal phase velocity of fluctuations cancels the poloidal component $\vec{ExB}$ of the parallel flow. This finding would mitigate against the idea of

transport of impurities from outer to inner target regions, by frictional coupling with fuel species, referred to above in [2]. However calculations from TTP data, [7], suggest that this cancellation does *not* take place on JET. Furthermore, LaBombard found that the maximum in the parallel flow was just 2mm outside of the separatrix, compared to 20mm outside, as measured on JET. However, this could be a function of the different SOL parameters (e.g. ρ^*, ν^*) on C-Mod and JET.

Mechanisms such as Pfirsch-Schlüter flow and Ballooning at the outer mid-plane were proposed in [1] as driving forces for the flow, however EDGE2D [8,9] modelling including $\vec{E}_{xB}$, $\vec{\nabla}B$ and centrifugal drifts did not predict the high values of Mach number measured in these or other researcher's experiments, [6,10]. The Mach number nearly always showed a maximum in the Scrape-Off Layer (SOL) at a radius of r ~ 10 to 25mm from the separatrix in mid-plane co-ordinates, as predicted by the model. However, an important finding was that when the field direction was reversed, the flow reversed but with a much smaller velocity, (M ~ 0.1), and showed a minimum rather than a maximum at r ~ 20mm. This was not predicted by the model, which suggested that the flow should reverse but have a similar value of Mach number, especially close to the separatrix. So the model predicted that if one takes the average of forward and reversed field parallel flow Mach numbers, the result should be close to zero, within 25mm of the separatrix – if field dependent forces, e.g. drifts, are mainly responsible for the flow. (It should be pointed out here that EDGE2D modelling as reported in [7,8] assumed very high temperature, low density plasmas – we will show here that the result is somewhat different when 'real' edge parameters are used).

Numeric simulations of ion orbit losses, [11], have also suggested that these may be responsible for flows in the SOL, through momentum transfer from orbit lost ions to background ions in the separatrix region. Using momentum sources predicted in [11], attempts have been made to model the large (M~0.5) flows observed in JET using EDGE2D. However, the momentum source is insufficient, and can only produce a flow with M< 0.1, [12]. So although the direction of momentum transfer was correct, it was concluded that this mechanism was probably not the primary cause of the large flows observed in the SOL, which occur at r ~ 20mm, rather than close to the separatrix (3 – 5mm) where orbit loss momentum is transferred.

In this paper we expand the preliminary results from [1] by presenting further more detailed measurements of parallel flow in JET forward, that is with $\vec{\nabla}B$ drifts downward towards the divertor, and reverse field discharges. (In JET, plasma current is reversed with field direction to preserve helicity). We compare results from two reciprocating probe systems, a retarding field analyser (RFA), [13], and the turbulent transport (fluctuation) probe (TTP), [16], in the same poloidal position at the top of the torus. We examine the effects of the magnitude of toroidal magnetic field, B_T, and also plasma density, $\bar{n}_e$, on the flow measurements. We also examine the effect of increasing neutral beam power in L-mode discharges. Finally, we present results from modelling (EDGE2D *with drifts*) in which both field direction and puff rates of deuterium and impurities (carbon) have been studied using separate grids constructed for each specific experimental discharge.

2. THE PROBE SYSTEMS USED FOR PARALLEL FLOW MACH NUMBER MEASUREMENTS

A detailed description of the Retarding Field Analyser used on JET is described in [13]. This system is positioned at the top of the torus just outboard of the plasma centre line at a major radius of 3.25 m. It can reciprocate vertically to the separatrix region from a distance of 100 mm above the plasma in a time period of 200ms. When used as a Mach probe, slit plates positioned at right angles to the field lines on either side of the probe body are biased at ~–150volts to collect ion saturation currents, j_{sato} and j_{sati}, on plates facing the outer divertor and inner divertor respectively, along the field lines. These slit plates, made of a titanium, zirconium molybdenum alloy which will withstand high heat loads, are positioned behind a boron nitride window, area 24mm^2, which defines the collection area. However, this type of construction restricts the flow to the slit plates because of charge neutralisation on the interior surfaces of the 7mm thick windows, [14]. The magnitude of this effect has been modelled using the XOOPIC code, [Gunn, 15].

Experiments using the Turbulent Transport Probe are described in [16]. This is a 9 pin probe, with 5 pins positioned on the top of a 5mm high boron nitride divide, which is at right angles to the field lines. These pins, together with 3 pins behind one side of the divide, are all made of graphite and are 1 mm diameter. A pin on the other side of the divide is 2.5mm diameter and faces the outer divertor in the forward field configuration. For parallel flow measurements, the pins on each side of the divide are biased at –200V to collect j_{sato} and j_{sati} . Any pin may be floated to record floating potential, V_f. It is normal to record V_f on at least one of the pins on top of the divide during flow measurements, and this gives information on the probe position relative to the separatrix, i.e. the shear layer.

Both probes are in the same poloidal position in the JET torus, but separated by 180º toroidally, see Fig. 1. Both probes have boron nitride bodies to which is applied a thin carbon coating, (maybe of great importance, see later), and have an overall diameter of 40mm.

Two systems of data acquisition are used, a slow system with a 10kHz collection rate and a fast system which uses 500kHz digitisers. Both systems are used with the TTP, but only the slow system with the RFA.

In addition to the normal mode of operation with a fixed negative bias on the Mach probe elements, the TTP elements may have a voltage sweep at 100Hz to record Langmuir I/V characteristics. From these, electron temperature profiles, $T_e(r)$, may be derived. Ion temperature profiles are measured by the RFA.

3. EXPERIMENTAL MEASUREMENTS OF PARALLEL FLOW

3.1 COMPARISON BETWEEN PARALLEL FLOW MEASUREMENTS USING DIFFERENT PROBES

Both the RFA and TTP probe systems were used to measure parallel flow in the steady state region of ohmic and neutral beam heated discharges in which the density was stepped up during the discharge, and in discharges with a slow ramp in toroidal field, (0.06 T.s^{-1}). Up to 4 measurements

were made at 2 second intervals during each discharge. In this section a comparison between measurements using the two different probe systems, the RFA and the TTP, will be presented. For a toroidally symmetric plasma results might be expected to be the same, but this is not the case, as shown below.

Typical measurements of j_{sat} on each side of the probes are presented in Fig. 2. This example is for a 2 MA, 2 T normal field ohmic discharge with a central density ramp from $<n_e> = 1.6\ 10^{19}\ m^{-3}$ to $3.4\ 10^{19}\ m^{-3}$. Although measurements are made with the probe moving vertically into the plasma at R = 3.25m (see Fig. 1), all SOL profile results in this paper are mapped to the outside mid-plane and are presented in these co-ordinates. There is an uncertainty in the absolute position of the separatrix, which will be discussed later.

At first sight the agreement between measurements of j_{sato}, probes facing the outer divertor along the field line, and j_{sati}, probes facing the inner divertor, for each probe system is poor. However, the reasons for this discrepancy are understood and are due to the loss of ions to the walls of the RFA apertures, [14]. Also, the TTP separatrix position had to be moved relative to that of the RFA to match the change of e-folding length (the break between 'near SOL' and 'far SOL' seen at ~20 mid-plane mm on JET). Reasons for these discrepancies will be discussed later.

Parallel flow Mach numbers were calculated using Hutchinson's formula [17] as used in [1]:

$$M(r) = 0.4 \ln(j_{sato}/j_{sati}). \qquad (1)$$

The value of the pre-logarithmic constant is closely similar to that used by other researchers for Mach measurements, e.g. [6,10]. This pre-logarithmic constant is a function of plasma viscosity in the SOL, and falls as viscosity increases [17], so could possibly be somewhat in error (lower) if the SOL has a high carbon concentration, (assuming carbon plasma has a higher viscosity than a hydrogenic one). However, this is conjecture because little is known about the viscosity of the hydrogenic plasma let alone that of one containing carbon impurities.
In any case, Hutchinson suggests that the pre-logarithmic constant is not a strong function of viscosity.

Parallel flow Mach number profiles, derived from the measurements presented in Fig. 2 for both the RFA and TTP probes, are shown in figure 3. The results are shown separately for clarity – the profile shapes M(r) from each probe system are similar, with the absolute magnitude slightly higher for the RFA. Otherwise, the agreement is good, (remarkable, in fact, considering the uncertainties in flux to the two probes)! No error bars for the RFA experimental data are presented here because these are direct measurements of current to probe tips. The TTP is voltage scanned and the error bars here depict the Langmuir probe fits. Note that the TTP does not go in as far as the RFA in this example.

Note the shift in the maximum of the flow velocity to larger radii as the density increases. This is clear in the RFA data, but not so clear for the TTP which did not travel as far towards the separatrix. This observation will be discussed later.

3.2 MEASUREMENTS IN FORWARD AND REVERSE FIELD

Measurements comparing the RFA and TTP reported above do not quite reach the separatrix. However, measurements at constant plasma current, 2MA, but varying toroidal field, i.e. varying safety factor, using just the RFA to obtain parallel flow Mach number have been made. Central line average density, $<n_e> = 1.8\ 10^{19}\ m^{-3}$. Average j_{sat}'s to each side of the probe during identical discharges in both normal and reverse field operation are shown in Fig. 4, and the parallel flow Mach number in figure 5.

Several observations can be made. The first is that there is no change in parallel flow Mach number as the toroidal field is changed from 1.6 to 1.9T. The second is that the flow remains almost always in the same direction, independent of the field direction, although it is virtually stagnant in reverse field in the region where the normal field flow is a maximum. Note that positive values of M(r) indicate a measurement of flow at the probe in the direction outer to inner divertor.

The curve at M(r) ~0.2 is the difference (smoothed) between the forward and reverse field measurements.

3.3 THE EFFECT OF DENSITY ON PARALLEL FLOW MACH NUMBERS IN THE SOL

Discharges in which the central density, $\bar{n}_e$, was increased in 4 steps, coming into equilibrium in < 2s after each increase in D_2 gas puff rate, were used to record parallel flow as a function of density. All measurements shown in Fig. 6 are for 2MA, 1.76T ohmic discharges.

During these measurements it was observed that some discharges later in the day gave slightly different parallel flow Mach numbers to earlier ones, indicating probably that wall conditioning was playing a role. However, the general trend shown in Fig. 6 was observed, i.e. an increase in Mach number in reverse field and a slight decrease in forward field with increasing density.

We often assume that ion temperature in the SOL is twice the electron temperature (which is often the case from Onion-Skin modelling [18]), and this is generally not far from values obtained from measurements using the RFA. This is a reasonable assumption for the density range covered in this paper. However, good RFA measurements of T_i, especially close to the separatrix, are limited, (see [13]). Also, the TTP has to be operated with a sweep voltage on pins to obtain measurements of T_e, which is not the normal mode of operation for turbulent transport measurements. So temperature measurements in the SOL are difficult together with parallel flow measurements, for which the RFA is normally used. However, the TTP does normally measure floating potential, which we have found for many discharges on JET, including H-mode, is related to T_e. The relation ship between average T_e to both sides of the TTP in scanning mode is shown in Fig. 7.

The solid line is the theoretical floating potential (V_{fth}) from Stangeby, [19], together with a constant offset in V_{fth} of V_c = 17volts, namely:

$$V_{fth} = 0.5T_e \ln(m_e / m_i (T_i / T_e)(1-\delta)^{-2} + 0.5T_e + V_c \qquad (2)$$

where δ is the secondary electron coefficient. The best fit to the data is when a ratio $T_i/T_e = 2$ is chosen (for $\delta = 0.3$), however $1 < T_i/T_e < 5$ just about bounds the data. Since [19] is with respect to plasma potential, this constant offset of ~17 volts suggests a relatively constant plasma potential for all discharges. A somewhat similar result was found in [20] for the DITE tokamak, in which sheath potential was plotted as a function of T_e.

The relationship is only accurate to about a factor 2 in T_e at the separatrix and across the SOL. However, since T_e appears as a square root in ion sound speed,C_s, the relationship is generally useful.

Measurements of $T_e(r)$ from the scanning TTP probe, from normal field shots as shown in Fig. 2, are shown for both ion and electron sides in Fig. 8. At the lowest densities T_e's are similar on each side, but somewhat lower on the side facing the outer divertor at the higher densities. Results from eq.2 show a good match to the data from the probe facing the outer divertor.

It is useful, for comparison with other tokamaks, to establish the collisionality regime in which we are working for these discharges. Exact evaluation of density in the SOL from the probe data is difficult, but we can assume that Lithium beam data, presented later, is correct at least to within a factor 2. So at the separatrix, for the lowest density discharges presented here, collisionality $\nu^* \approx 20$, and for the highest density discharges $\nu^* \approx 10$. ν^* rises rapidly as we go further into the SOL, so for low density $\nu^* \approx 67$ at 10mm from the separatrix, and $\nu^* \approx 46$ for the highest density case. These figures assume no impurity (Z = 1) and could be higher in the presence of carbon impurity.

From the floating potential and electron temperature profiles the radial electric field has been calculated classically as:

$$E_r = -\partial / \partial r(V_{f\,\exp} + 2.5T_e) \qquad (3)$$

E_r calculated for the lowest and highest densities in figure 8, using experimentally measured values of floating potential, V_{fexp}, is shown in Fig. 9. Unfortunately data is only good enough in normal field discharges to allow taking the derivative, as in (3).

The result indicates that E_r increases more rapidly at the higher density, but only approaches values of 3kV.m^{-1} near to the separatrix. This result demonstrates how the electric field increases at any given radius as the density increases.

It is useful to distinguish at this point between Mach number, which is related to the parallel flow velocity v_{ll}, $v_{ll} = C_s M$ and total flow of particles, which may be responsible for the transport of carbon from outer to inner divertor, for example, by frictional coupling. The parallel flow velocity is perhaps a more physically useful parameter than the Mach number, but its derivation at first sight requires a knowledge of ion and electron temperatures, T_i , T_e. (In fact, as shown later, C_s is *not* required to obtain v_{ll} , but is used in other analysis).

$$C_s = \sqrt{\frac{e(T_e + T_i)}{m_i}} \qquad (4)$$

We define the parallel flow of particles here as:

$$\Gamma_{\|} = n_e C_s M \tag{5}$$

where $n_e(r)$ is the local density and C_s the ion sound speed. However, this is not necessary for calculation of $\Gamma_{\|}$ since:

$$2 j_{sat} = e n_e C_s \tag{6}$$

Hence Γ_{ll} can be calculated directly from results of Fig. 3.

$$\Gamma_{\|} = 2 j_{sat} M / e \tag{7}$$

In Fig. 10, the parallel flow of particles across the SOL is plotted.

3.4 THE EFFECT OF NEUTRAL BEAM POWER ON PARALLEL FLOW MACH NUMBERS IN THE SOL OF L-MODE AND H-MODE DISCHARGES.

The power to the plasma was increased using neutral beam injection from ohmic (1MW) up to > 5MW in 4 steps during similar discharges in forward and reverse field, and the reciprocating probes inserted towards the end of each step when the plasma was in equilibrium, (dW/dt ~ 0). Plasmas were generally L-mode, 2 MA, 2.4 T. In the parallel flow Mach number profiles shown in Fig. 11, the highest total input power (5.1MW) shown for forward field has just gone into H-mode, (very low frequency ELMs which do not occur in the time period of the reciprocation). In reverse field, for the highest total power (5.3MW), the plasma is still in L-mode. The rapid rise in Mach number for r > 40 mid-plane mm. corresponds to low levels of j_{sat}, and as such may be unreal. Note that although the aim of this experiment is to examine the effect of power on flow, $\bar{n}_e$ also increases as a result of the neutral beam, as shown in Fig. 11. Clearly the conclusion from the RFA data shown in Fig. 11 is that there is little change in M(r) with increasing power, both in normal and reverse field configurations.

4. CODE SIMULATION OF THE PARALLEL FLOW MEASUREMENTS USING EDGE2D

Some preliminary EDGE2D modelling with $\vec{E}\vec{x}\vec{B}$, $\vec{\nabla}\vec{B}$ and centrifugal drifts were reported in [1]. However, to get the values of Mach number M(r) as high as ~ ±0.2 shown in Fig. 8 of [1], very high target temperatures (i.e. a very hot, low density plasma) had to be assumed. Similar code simulations with drifts have been made using UEDGE, [21], on JET and other machines, and these also suggested that the Mach number should be much smaller than that measured experimentally in the low field side SOL. In this paper we will try to match target densities and temperatures as predicted by

EDGE2D to those measured by probes in the divertor targets, $n_{et}(r)$ and $T_{et}(r)$. Usually, if a reasonable match between code prediction and experiment is obtained for these downstream (target) parameters, then upstream (SOL) $n_{eu}(r)$ and $T_{eu}(r)$ as measured by the Reciprocating probes are also matched as well, since upstream parameters are quite robust compared to target parameters, [22]. In addition to this, separate grids for the EDGE2D modelling have been constructed from the experimental discharges under investigation, for both forward and reverse field situations. A generic grid was used in [1].

In an attempt to understand the high experimentally measured values of M(r), compared to the low values obtained using the code, the simplest situation of an Ohmic plasma has been modelled, but including the effect of increasing density. In other words, modelling of the experimental results shown in figure 6 was attempted.

The plasma modelled was 2MA, 1.76T, and deuterium puffing from the top of the torus was used, as in the experiment, to control the density. Experimental puff rates were up to 10^{22} $D_2.s^{-1}$, but as is usual the code required a factor 3 – 4 less, 1.2 to 3 10^{21} s^{-1}. Wall pumping is a possibility for this discrepancy, although this is a feature of vertical target operation, (see figure 1). When the plasma separatrix is on the horizontal target, puff rates of up to 10^{22} $D_2.s^{-1}$ are indeed required by the code. The total input power for these discharges was 1.6 MW, and of this 1 MW was assumed to go into the ion channel and 0.6MW into the electron channel in the code.

$\vec{\nabla}B$, $\vec{E}\times B$ and centrifugal (curvature particle) drifts were switched on for both deuterium and impurity (carbon) species in the SOL, including radial, parallel and transverse components. Carbon chemical sputtering was included as indicated in measurements by Haasz, [23].

Cross-field diffusion coefficients are often considered constant in edge plasma modelling, but DIVIMP-OSM [18] modelling of similar plasmas to these indicate that the thermal diffusivity, $\chi_\perp(r)$, often increases with r in the SOL to reach a maximum at ~ 20 mid-plane mm. This has been confirmed experimentally for the particle diffusivity, $D_\perp$, by measurements and fluctuation analysis, using the TTP, [24]. Generally is it assumed that $D_\perp(r) = 0.4\,\chi_\perp(r)$, [25]. Also indicated in [18] was that for low power ohmic plasmas $\chi_\perp(r)$ is quite high (~1) and reasonably constant compared to higher power discharges – the TTP suggests values of $D_\perp > 3 m^2.s^{-1}$ and a stronger variation with radius. In view of these experimental findings, a value of $D_\perp = 0.5\ m^2.s^{-1}$ close to the separatrix was chosen for these code runs, rising to $D_\perp = 1.5\ m^2.s^{-1}$ at r = 20 mid-plane mm. $\chi_\perp(r) = 2\,D_\perp(r)$was also assumed. The code does not appear too sensitive to changes (factor of 2) in these coefficients.

4.1 SIMULATION OF THE REVERSE FIELD MEASUREMENTS

Measurements in reverse field, Fig. 5, show a clear overall increase in M(r) towards the inner divertor with increasing density, indeed at the highest densities flow is almost totally in this direction across the SOL. An example is shown in Fig. 12 of the EDGE2D simulation of the target profiles of $n_{et}(r)$ and $T_{et}(r)$, again referred to the mid-plane. This is for the low density

case, $<n_e> = 1.7\ 10^{19}\ m^{-3}$. Distances in Fig. 12 shown as negative are in the private flux region.

Fitting is to the outer SOL T_e data by controlling the gas puff from a gas source near the top of the machine. The agreement with density in the outer divertor is within a factor 2, (good in view of field line angle and area effects to the target probes). Agreement with inner divertor data is also good for reverse field discharges. Note that the private region (shown as $r < 0$) match is poor – the private region cannot be mapped to the outside mid-plane in a satisfactory manner. The measured parallel flow Mach number is plotted in Fig. 13a, and that predicted by EDGE2D is plotted in Fig. 13b. Note that in this plot although the general trend with both radius and density appears good at first sight, the predicted Mach number is too low by a factor 5.

The accuracy of the JET magnetic equilibrium reconstruction code EFIT [26] is only a few tens of mm. at the reciprocating probe positions at the top of the machine, due to a low density of coils in this region. However, near the target probes the situation is much better and an accuracy of a few mm might be expected.

4.2 SIMULATION OF THE FORWARD FIELD MEASUREMENTS

Measured density and electron temperature profiles across inner and outer target for the forward field situation are shown in Fig. 14, together with the EDGE2D simulation. Again we choose the low density case, $<n_e> = 1.8\ 10^{19}\ m^{-3}$. Here again the code prediction is good for the outer divertor, but temperature predictions for the inner divertor are very low compared with experiment, hence densities somewhat high, ($n_{et} \propto J_{satt} / \sqrt{T_{et}}$). This is the major difference between the normal and reverse field simulation – we cannot match the inner divertor temperature in normal field. Note that again the fitting has been done for best fit to outer divertor $T_e(r)$ rather than $n_e(r)$, since the latter has uncertainties in j_{sat} measurements as described in 4.4. Puff rates required in the code simulations are in fact the same for both normal and reverse field runs.

The unperturbed ion saturation current to the probe, i.e. corrected for the measured flow by using Hutchinson's fluid model, [17], can be approximated by:

$$\Gamma_0 = \Delta\Gamma + 0.1 * \sin(2.3813 * \Delta\Gamma) \tag{8}$$

$$\text{where } \Delta\Gamma = j_{sato} - j_{sati} \tag{9}$$

This simple function proves to be accurate to better than 0.1% for all M!

Γ_0 has been calculated from (8) from the RFA data, and plotted together with the EDGE2D prediction in Fig. 15. The RFA j_{sat} data has to be multiplied by a factor 5.5 to match the code prediction, but otherwise the match is excellent. Note in particular the break to a second SOL at r = 10 – 20 mid-plane mm, then back again to approximately the original slope in the far SOL.

The EDGE2D predicted parallel flow at the reciprocating probe position is compared with the experimental measurements in figure 16. The code predictions have been multiplied by a factor 5 to

allow presentation on the same plot. For forward field the experimentally measured flow is about an order of magnitude higher than the code prediction, and the general shape of M(r) is in disagreement with the code. However, there is not much change in M(r), either in code prediction or experiment, with increasing density.

Possible reasons for this disagreement between code prediction and experiment are discussed below.

4.3 SEPARATRIX POSITION

Knowledge of the separatrix position is important for comparison of probe data with that of other diagnostics, and also to match the code results of M(r) with experiment. There is often some problem in defining the separatrix position when presenting SOL data from the reciprocating probes. As stated above, it is believed that errors in the separatrix position as predicted by EFIT can be as much as 20 mid-plane mm. To this there should be added an uncertainty in the absolute height of the probe, which is unknown, but could be as much as 10 mid-plane mm. Unfortunately there are often no clear changes in e-folding lengths of density or electron temperature at the separatrix, (although 'near' and 'far' SOL's with different e-folding lengths can be used, as in fig.4, to match profiles from the two systems). So the choice of absolute position can be in error by the distances indicated above, or we can get a better idea by using data from diagnostics which are in the target tiles, (Langmuir probes), which are closer to pick-up coils. The signals to use here are the target flux density, j_{satt}, and temperature, T_{et}. However the maximum in j_{satt} should be used as an indicator of the separatrix position rather than T_{et} which often falls close to the separatrix, yet remains high in the far SOL.

Electron pressure balance between the outer target and the reciprocating probe position is used here as a check on separatrix position. In fact, since we believe that we have not reached the separatrix during some reciprocations, pressure balance is made at r~7 mid-plane mm. It is acknowledged that this technique could be in error at high densities close to target detachment, which may be true at the inner target and close to the separatrix at the highest densities reported here, and also because the flow itself will modify the pressure balance somewhat. However, the aim is simply to get an idea of the separatrix position using target probes, since from EFIT the position is known to within a few mm accuracy along the targets. Basically, we assume:

$$n_{eu}T_{eu} = 2n_{et}T_{et} \qquad (10)$$

This was done initially for intermediate density shots, outer target, and an error in EFIT upstream compared with target position of 22mm was found. However, this error increases at lower densities, and decreases at higher densities, as shown in figure 17. This could either be a real movement in the plasma separatrix, not recorded by EFIT, or simply an error in the EFIT reconstruction, which varies with density.

The electric field in the plasma changes rapidly close to the separatrix, so a second method

which gives an idea of the separatrix position is to examine the shear layer using measurements of floating potential, V_f, and deduced electric field, E_r, as shown in figure 9. Unfortunately it is uncertain just where in the shear layer the separatrix occurs, although one might expect it to be close to the position of maximum E_r. On some discharges where the probe has gone further in to the plasma, E_r falls again towards zero, but it is uncertain whether this is due to a fall in E_r inside the separatrix, or electron emission from the probe tip.

On the basis of these measurements, one could assume that the separatrix position actually moves out with increasing density. However, this is uncertain and could simply be due to a change in the magnetic reconstruction with density. So in all the data plotted above, for clarity, the separatrix position is assumed independent of density with a constant offset of EFIT + 22mm.

4.4 COMPARISON WITH OTHER DIAGNOSTICS

The comparison of j_{sato} and j_{sati} for the RFA and TTP as shown in figure 2 indicates that the collected currents are very different on the two probe systems. The obvious question is how do the densities as measured by the RFA and TTP compare with other edge diagnostics? In many discharges there are simultaneous measurements of density using a Lithium beam and Edge Lidar. Densities from the RFA and other diagnostics are shown in figure 18. The RFA density was derived from J_{sato} and an average T_e (r) as measured by the TTP.

The RFA density is low by a factor 6 – 10 times compared with the Lithium beam and the few points from the Edge Lidar. Also, the 'near' and 'far' SOL regions as measured by the probes are not clearly shown as changes in e-folding length on the Lithium beam data, which generally only shows a single SOL. This disagreement between probe and Li beam data suggests that the probe may be influencing the measurements.

The RFA has 6mm x 4mm windows in 7mm thickness boron nitride, behind which are the slit plates used for j_{sat} measurements. Runs of the XOOPIC code, [14], for 5mm and 4mm diameter 'tunnels' indicate that an attenuation of flux of just about this order is expected, due to cross-field transport on to the interior walls of the hole.

The density as derived from the TTP is about a factor 2 low compared with the Lithium beam, which is not unreasonable considering area uncertainties for the TTP pins due to Larmor radii effects, and positional uncertainties in both diagnostics.

5. DISCUSSION

5.1 BALLOONING AS A POSSIBLE MECHANISM FOR INCREASED M(R)

The results for parallel flow Mach number presented here show a significant difference to the preliminary results presented in [1]. A common feature of all measurements is a rise in Mach number in reverse field close to the separatrix (in the shear layer as depicted by V_f(r)), and a fall close to the separatrix in forward field. At the separatrix, both forward and reverse field Mach number ~ 0.2. This is true for both increasing density discharges, Fig. 6, and those with increasing

neutral beam power up to H-mode, Fig. 11. In the earlier work this feature was not clear – the flow appeared to be close to zero at the separatrix. The reasons for this discrepancy are probably the superior statistics available from the present RFA and TTP probes (data rates of 10kHz and 500kHz respectively), compared with the 100Hz obtained with the voltage scanned Langmuir probes in [1], and secondly the fact that a completely different probe head was employed, i.e. a Mach probe rather than an RFA or TTP, (see later where we suggest that the probe itself might be responsible for inducing a flow).

In the preliminary study, [1], Ballooning transport was proposed as a possible mechanism for the high Mach numbers measured in the SOL, but then dismissed as it was difficult to explain the peaked structure of M(r), and difficult to see how the effect could almost vanish at the separatrix. However, this may not be the case in the light of the present measurements with M ~ 0.2 close to the separatrix.

Other investigators, for example results from C-MOD, [21], and JT-60U, [10], do not see this field independent offset in Mach number close to the separatrix. However, in C-MOD the horizontal scanning probe is just above the outside mid-plane position, and on JT-60U it is just below the outside mid-plane. So both of these investigators have probes close to the hypothetical stagnation point of the poloidal flow. Ballooning tends to be greatest at the outside mid-plane where field line curvature is highest. There will be no gradient driving a parallel flow due to ballooning close to the maximum ballooning position in these machines, however on JET the probe is well above the mid-plane, where a strong gradient may exist.

Consider that the total flow, $M_t(r)$, is made up of two components, one due to drifts and dependent on the field direction, $M_d(r)$, and the second independent of field, $M_b(r)$. So that in the forward field direction:

$$M_{tn}(r) = M_d(r) + M_b(r) \tag{11}$$

The EDGE2D runs presented in [1] show that, at least for r < 25 mm, the flow due to drifts is almost symmetric about zero. So in the reverse field direction:

$$M_{tr}(r) = -M_d(r) + M_b(r) \tag{12}$$

Adding (6) and (7) gives the field independent term:

$$M_b(r) = (M_{tn}(r) + M_{tr}(r))/2 \tag{13}$$

i.e. the average of the two plots shown in Fig. 5. $M_b(r)$ has been included on this plot, and it is clear that this 'extra' mechanism is almost independent of radius.

If we assume that Ballooning is responsible for the increased flow, this gives us a slight problem.

Assuming that there are no ionisation sources in the SOL, and no return flux to the core, then the total particle flux coming out of the core must equal that flowing past the reciprocating probe and eventually reaching the inner divertor. Making these assumptions, we can check on whether the flux coming out of the core, which is calculated by EDGE2D, is sufficient to account for the flux we measure (in Fig.10, for example). The code predicts a total outflux $\Gamma_T = 4.10^{19}$ $m^{-2}.s^{-1}$, i.e. a predicted D_α photon flux of 3.7 10^{13} photons.s^{-1}.cm^{-2}.sr^{-1} compared with a measured horizontal D_α photon flux of 6.4 10^{13} photons.s^{-1}.cm^{-2}.sr^{-1} for this reciprocation. Some poloidal asymmetry might be expected, (less outflux on the high field side), hence the comparison is reasonable.

To account for the loss rate due to the flow, Fig. 10 has been integrated across the SOL. The loss rate is 6.9 10^{20} $m^{-2}.s^{-1}$. This is over an order of magnitude higher than is possible from the code prediction, even assuming that all the flux passes the probe position! So the D_α photon flux and code predictions agree, but the probe result from the flow does not. We can imagine a situation where the flux we measure is smaller (the flux is integrated along the flux tube), but not much higher than that coming from the core. The situation would be resolved if the 'real' Mach number was that which is predicted by EDGE2D, namely M ~ 0.05. This is strong evidence that the probe results for flow are too high.

We are left with the possibility that Ballooning could be one field independent mechanism driving the flow, but the argument is not entirely convincing, because of the measured high value of M ~ 0.2 across the SOL.

We mentioned in the introduction that one result, which suggested a substantial flow from outer to inner divertor regions, was the large build-up of carbon on the inner divertor louvers, [2]. For this to happen, the flow must be poloidal rather than purely toroidal, which would not effect transport down into the divertor. From the results for E_r presented in Fig.9, the poloidal velocity may be calculated, as $V_p = \vec{E}_r \times \vec{B}_\theta$. These data are presented in Fig.19 for two different densities in normal field, with the EDGE2D predicted poloidal velocity at approximately these densities plotted on the same figure. The shape of the code prediction matches quite well, but the code predicts a stagnation and indeed a reverse poloidal velocity just outside of the separatrix. We don't know how large V_p should be to carry impurities to the inner divertor, but the fact that the experimentally measured flow is always in the correct direction suggests that this flow could be responsible. Note that no attempt should be made to extrapolate the experimental data shown here to the separatrix, as there is some suggestion from other discharges that the curves flatten inside the radii shown. The results suggest measured poloidal flow velocities much less than measured parallel velocities.

Yet another mechanism might be amplifying the field dependent and independent components of the flow and creating the high parallel flow Mach numbers measured here.

5.2 DOES CARBON RADIATION EFFECT FLOW?

5.2.1 Between Targets

Another possible mechanism for the additional 'extra' parallel flow, i.e. over and above that due to

drifts and predicted by EDGE2D, is a flow induced by an energy sink downstream of the probe. This could occur between targets if there were a large temperature difference between plasmas at the end of field lines at each target, such as might result from high impurity radiation. Interestingly, however, for the case of forward field during which the highest flows are measured, the inner target in fact shows a similar $T_e(r)$ to the outer target. Also radiation at the inner target is generally similar to, or even lower than that at the outer target (in contrast to the EDGE2D prediction). This would drive a flow in the wrong direction to that measured. The pressure at inner and outer targets is also similar, so it is doubtful that a flow can be driven between targets due to a pressure gradient.

Certainly EDGE2D *does* predict an increase in flow with reducing density (which was how flows a high as ~ 0.2 in the outer SOL were predicted in our earlier code runs of [1]). Figure 12 shows that experimentally there is *not* much change in M(r) with density, however. If the flow is indeed pressure driven, then it is more likely that pressure differences are occurring much closer to the probe.

5.2.2 In the vicinity of the probe

One possible explanation is that the carbon is being sputtered from the body of the probe itself, then radiating and cooling the plasma locally downstream of the probe.

This mechanism needs a flow to start with, a flow which is amplified by an increasing radiation sink and hence an increase in flow – a bootstrap effect. Using the colour CCD camera, a large white plume, presumably carbon radiation, is seen extending in the direction towards the inner target. The extent of the plume in forward field discharges on the other side of the probe is smaller. However, in reverse field discharges, the extent of the plume is similar in each toroidal direction. Frames from the CCD camera are shown in Fig. 20, for forward and reverse field discharges. Careful measurement of the CCD images shows that the probe itself in forward field is well to the right in the bright carbon plume, compared with that in reverse field.

Observation of ‘plumes’ during a helium or nitrogen gas puff from a reciprocating probe in Alcator C-Mod, [27], have been made. However, it was concluded from code simulations that quantitative information on parallel flow velocities was not robust at low ionisation states, (where the impurities are not fully thermalised).

Using published data for ionisation cross-sections for carbon, [28], the mean free path, λ, for a carbon atom sputtered from the probe surface near to the separatrix (T_{eu} = 25 eV, $n_{eu} = 6\ 10^{18}\ m^{-3}$) in these discharges is ~ 8mm. Further out in the SOL, at the peak of the M(r) profile, (T_{eu} =14 eV, $n_{eu} = 1.2\ 10^{18}\ m^{-3}$) $\lambda \sim$ 75mm. Such a gap would not be seen in the views above, however, as the probe would be surrounded by light.

We have attempted to model this carbon radiation downstream of the probe using EDGE2D, however the problem is 3D, and we are using a 2D code, so quantitative simulation is impossible. A carbon source cannot be simulated directly in EDGE2D, however the radiation can be simulated by situating an energy sink distributed radially in the SOL but peaking close to the separatrix, and

at one ‘row’ of the grid used in EDGE2D downstream of the probe. Because the energy sink causes a density build up, a particle sink can also be applied to reduce somewhat this density build up. However, even with the particle sink, there is still a density build up and a parallel density gradient which is positive from the position of the probe to the position of the sink exists. This density gradient would be expected to reduce the flow towards the inner target, but the temperature at the sink falls as well, and as can clearly be seen in Fig. 21 the overall result is an increase in Mach number towards the inner target. The radial distribution of the sink is chosen to match the experimental Mach number profile. This is difficult to justify, although the plume downstream of the probe shows roughly this radial distribution, rather than a maximum in light emission close to the separatrix.

The increase in the flow velocity above that obtained with no energy sink is dramatic in figure 21, even with no particle sink. The parallel flow Mach number increases to a value M(r) ~ 0.16 near to r ~ 20mm, or 0.25 with the additional particle sink. Both the shape and magnitude of the profile approximates well to the measured experimental result for this discharge (if one includes the constant field independent component), but note the caveat above re- magnitude. The result could mean that the probe amplifies the SOL flow it is trying to measure, by carbon sputtered from its surface streaming away at high velocity.

EDGE2D clearly shows the differences in T_{eu} at the probe position and just downstream with this energy sink. If z is the distance along the field line from the probe, then $-dT_{eu}/dz = 0.0$ upstream of the probe, and $dT_{eu}/dz = 0.1$ eV.m^{-1} downstream of the probe, so a very small temperature gradient is all that is required to drive this large flow. The flow is down the gradient, rather than up as would be expected, because of the higher mass carbon impurity.

It is suggested here that the carbon sputtered from the probe surface ionises and lowers the plasma temperature by radiation downstream of the probe, as observed experimentally with the CCD camera. Certainly CIII light along a vertical chord looking down into the divertor often shows a rapid rise during probe reciprocation, despite the very high background light level coming from the divertor itself. To cause this toroidal asymmetry in carbon light near to the probe there must be a flow to start with. This is then amplified as carbon moves downstream, radiates, and lowers the temperature of this downstream region further, thus increasing the flow.

Further evidence for the involvement of carbon in the probe measurements is exemplified in Fig. 22. Here we plot the upstream density profiles as obtained from EDGE2D runs, (the low density case, $\langle n_e \rangle = 1.6\ 10^{19}$ m^{-3}). To match the density profiles as recorded by the probes, (most clearly shown by the j_{sat} profiles of Fig. 4), a $D_\perp$ (r) profile as shown in Fig. 23 is required, i.e. having a maximum around r ~ 20mm. This results in the clear ‘near’ and ‘far’ SOL e-folding lengths nearly always recorded by the probes. Such ‘double SOLs’ are also seen on C-MOD, [31], however the ‘kink’ in the density profile is much closer to the separatrix than observed on JET (~ 5 mm), a result which could be due to the smaller ρ* on C-MOD, due to higher field operation. On the other hand, the Lithium beam data for this discharge at this time shows no such ‘double SOL’. An EDGE2D run with constant $D_\perp$ shows much better agreement to the Lithium beam data. Also

shown in Fig. 22 is an example of a Lithium beam profile in which the 'double SOL' *is* seen. This has CD_4 injection. A profile taken 2 s later in the same discharge (with CD_4 pumped away, but D_2 injected to the same density) also shows a slight 'double SOL'. Note the 'break' in profile e-folding length is at exactly the same radius as the EDGE2D profile required to fit the probe data. The single SOL measured by the lithium beam, compared to the double SOL recorded by the reciprocating probe, is strong evidence that the probe is having an effect on the SOL.

Note that in the case where CD_4 is injected from the edge the Lithium beam profile only shows a single break to a second SOL. This is rather different from the probe result (perhaps more clearly shown in Fig. 15) where a break back again to the original e-folding length is seen in the far SOL. If the probe second SOL is due to carbon, then it might be expected, however, that carbon coming from the probe gives a different result to carbon coming through the SOL from the wall.

The only other currently available explanations for the high flow rates measured in the SOL are those of: a) turbulent transport driven flow (Hidalgo et al, using the TTP here at JET, [3]) . b) Toroidal rotation (as suggested by LaBombard, on Alcator C-Mod, [6]), and c) Ion orbit losses,[11].

a) Hidalgo et al. found that there was a strong coupling between turbulent transport and parallel flows, and concluded that flows were, at least partially, driven by turbulence mechanisms. However, it is difficult to prove that turbulence is responsible, i.e. whether it is a cause or an effect.
b) Evidence for toroidal rotation has not been observed on JET. The poloidal phase velocity is close to zero in the SOL increasing only inside the shear layer, so there is no cancellation of the poloidal phase velocity of fluctuations and the poloidal component ($\vec{E} \times \vec{B}$) of the parallel flow as observed on C-Mod. Also, there are strong differences between the results reported here and those obtained on Alcator C-Mod.

Parallel flows on C-Mod are found to peak at just 2mm from the separatrix, whereas the maximum is at ~ 20 mm on JET. Also, C-Mod returns an almost symmetrical reversal in flow when the field direction is changed, quite unlike JET.

c) On the basis of ASCOT code runs, Fundamenski et al. conclude that although flows are in the right direction to be driven by momentum transfer from orbit loss ions, the magnitude of this process is too small to be their primary cause.

Our experiments indicate that there is very little change in Mach number with increasing neutral beam power in L-mode discharges, and the variation with increasing plasma density is also small. However, as seen by other workers, [29, 30], there is a reduction in M(r) with increasing density, although the effect here (in forward field) is not nearly as much as seen on other machines. The interesting finding here is that the flow towards the inner divertor increases with increasing density in reverse field, suggesting that the field independent component of the flow is becoming more important as the density rises, as in normal field.

CONCLUSION

In this paper we have presented new and more detailed recent experimental data on plasma flows in the JET SOL with forward and reversed toroidal field and current. Scrape-off layers parameters for key discharges have been simulated using EDGE2D-U/NIMBUS with neo-classical drifts and transport parameters adjusted to give a best match to experimental profiles.

Two mechanisms have been proposed for the experimentally measured flows in the SOL. The first is a field independent mechanism, which from the difference between normal and reverse field measurements appears nearly constant at M ~ 0.2 across the SOL. The second mechanism is field dependent, and exhibits a reversal of the flow with reversal of the drift direction. Ballooning has been suggested as a possible field independent mechanism, an idea strengthened by our observation that this component increases with increasing density.

Unfortunately, EDGE2D with classical drifts predicts Mach numbers of up to an order of magnitude less than those measured experimentally, i.e. M(r) peaking at r = 20mm in normal field with a value of ~ 0.6, which is almost independent of most plasma parameters. Alternatives to classical drifts are discussed, and none appear to offer a consistent explanation for the high values of parallel Mach number measured.

An explanation for the relative invariance of M(r) with all plasma parameters in normal field is challenging. However, EDGE2D does suggest a qualitative independence of flow with density with this field direction. It is the magnitude of the measured flow that presents the problem.

With the help of EDGE2D modelling we have also explored the possibility that the high Mach numbers are an artefact due to impurities generated by the probe. Our idea is that the probe might be *amplifying* the flow velocity by radiation cooling of a region just downstream of the probe. If this idea is correct then Mach probes can be trusted only for determining the direction of the flow and not its magnitude. This then offers a way out of the problem that none of the physical processes so far studied seem able to reproduce the magnitude of the measured Mach numbers. However, due to the lack of a suitable 3D code, this analysis in not quantitative and so remains somewhat speculative. It is equally possible that there is some important physical process missing from EDGE2D and other similar edge fluid codes. Independent experimental validation of the probe measurements by a non-perturbing method is a clear experimental priority but is difficult to achieve in the region of the JET edge plasma which can be reached with a probe.

REFERENCES

[1]. Erents, S.K., Chankin, A.V., Matthews, G.F., Stangeby, P.C., Plasma Phys. Control. Fusion **42** (2000) 905-915.

[2]. Coad, J.P., Erents, S.K., Fundamenski, W., Matthews, G.F., Rubel, M., Strachan, J., in Proc. 28th EPS Conf.. Madeira, 2001.

[3]. "Experimental investigation of the dynamical coupling between turbulent transport and parallel flows in the JET plasma boundary region" Hidalgo, C., GonÁalves, B., Silva, C., Pedrosa,

M.A., Erents, S.K., Hron, M., and Matthews, G.F. Accepted for publication in Physical review Letters, 2003.

[4]. Pitts, R.A., Duran,I., Erents,S.K.,Horacek,J.and Matthews,G.F, Proc. 30th EPS Conf. On Contr. Fusion and Plasma Phys., St. Petersburg, 7-11 July 2003, ECA Vol. 27A, P-2.84.

[5]. Valsaque, F., Manfredi,G.,Gunn,J.P. and Gauthier,e., Phys. Plasmas **9** (2002) 1806.

[6]. LaBombard, B., Gangadhara, S., Lipschultz, B., and Pitcher, C.S., J.Nucl.Mater., 313 – 316 (2003) 995.

[7]. Silva, C., Laboratorio Nacional de Fusion, Euratom-Ciemat, 28040, Madrid, Spain. – Private Communication.

[8]. Chankin, A.V., *et al*., 1999 'Modelling of SOL flows and target asymmetries in JET field reversal experiments with EDGE2D code'. 7th Plasma Edge Theory Workshop (Tajimi, Japan, October 4-6, 1999).

[9]. Chankin, A.V., *et al*., 1999 'Modelling of SOL flows and target asymmetries in JET field reversal experiments with EDGE2D code'. 7th Plasma Edge Theory Workshop (Tajimi, Japan, October 4-6, 1999).

[10]. Asakura, N., sakurai, S., Itami, K., Naito, O., Takenaga, H., Higashijima, S., Koide, Y., Sakamoto, Y., Kubo, H., and Porter, G.D. J.Nucl.Mater., 313 – 316 (2003) 820.

[11]. Fundamenski, W., Sipila, S., Eich, T., Kiviniemi, T., Kurki-Suonio, T., Matthews, G. and Riccardo, V., J. Nucl. Mater. 313 – 316 (2003) 787.

[12]. Matthews,G.F., Corrigan,G., Erents,S.K., Fundamenski,W., Kallenbach,A., Kurki-Suonio,T., Sipila,S. and Spence J., J. Nucl. Mater. 313 – 316 (2003) 986.

[13]. Pitts, R.A., Chavan, R., Erents, S.K., Kaveney, G., Matthews, G.F., Neill, G., Vince, J.E., and Duran, I. Rev.Sci.Instrum. **74** (2003) 4644.

[14]. J. P. Verboncoeur, A. B. Langdon, N. T. Gladd, Comp. Phys. Comm. **87**, (1995). 199.

[15]. Gunn, J.P., Physics of Plasmas **8**, No.3 (2001) 1040.

[16]. Hidalgo, C., GonÁalves, B., Silva, C., Pedrosa, M.A., Silva, C., Balbin, R., Hron, M., Loarte, A., Erents, S.K., Matthews, G.F., and Pitts, R.J. Nucl. Mater., 313 - 316 (2003) 863.

[17]. Hutchinson I. H., Phys. Rev. A37 (1988) 4358.

[18]. Erents, S.K. and Stangeby, P.C., Nucl. Fusion 38, No. 11 (1998) 1673.

[19]. Stangeby, P.C. 'The Plasma boundary of the Magnetic Fusion devices" IoP Publishing Ltd, 2000. ISBN 07503 05592.

[20]. Pitts,R.A. and Matthews,G.F., J. .Nucl. Mater. (176 – 177) (1990) 877.

[21]. Porter, G.D., Rognlien, T.D., Rensink, M.E., et.al., J.Nucl. Mater. 313 – 316 (2003) 1085.

[22]. Erents, S.K., Stangeby, P.C., LaBombard, B., Elder, J.D. and Fundamenski, W., Nucl.Fusion **40** No.3 (2000) 295.

[23]. Haasz, A.A. and Davis, J.W., J. Nucl. Mater, (1996) **219**.

[24]. Matthews, G.F, Corrigan, G., Erents, S.K., Fundamenski, W., Mailloux, J., Spence, J., Pericoli, V., Strachan, J., Garcia-Cortes, I., Hidalgo, C., Pedrosa, M.A., and Silva, C., 28th EPS Conf. On

Contr. Fusion and Plasma Phys. Funchal, 18-22 June 2001, ECA Vol 25A (2001) 1613-1616.
[25]. LaBombard, B., et al., in Fusion Energy 1996 (Proc. 16th Int. Conf. Montreal, 1996), Vol. 1, IAEA, Vienna (1997) 825.
[26]. EFIT Home Page: http://fusion.gat.com/efit/
[27]. LaBombard, B., Gangadhara, S., Lipschultz, B., et.al., J.Nucl. Mater. 266-269 (1999) 571.
[28]. Freeman, R.L. and Jones, E.M., Culham Laboratory Report CLM-R 137, May 1974.
[29]. Asakura, N., Sakurai, S., Shimada, M., et. al., Nucl. Fusion, **39** (1999) 1983.
[30]. LaBombard, B., Goetz, J.A., Hutchinson, I.H., et.al., J. Nucl. Mater. 241 – 243 (1997) 149.
[31]. LaBombard, B., Umansky, M.V., Boivin, R.L., et.al., Nucl.Fusion, **40** (2000) 2041.

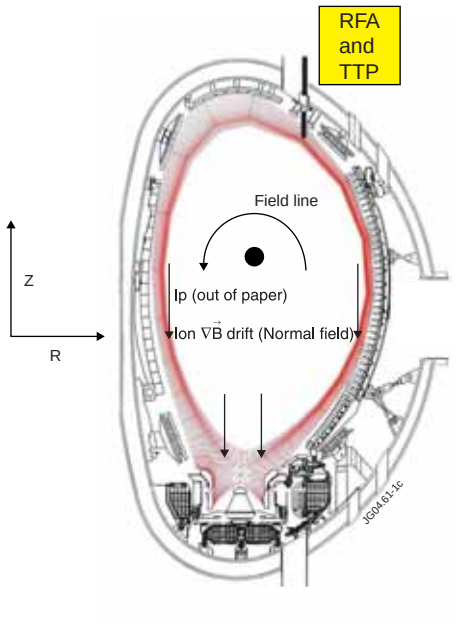

Figure 1: Poloidal view of the JET torus showing position of Mach probes. Both RFA and TTP probes are in the same poloidal position, but 180º apart toroidally. The grid shown in the figure is a typical grid used in EDGE2D modelling.

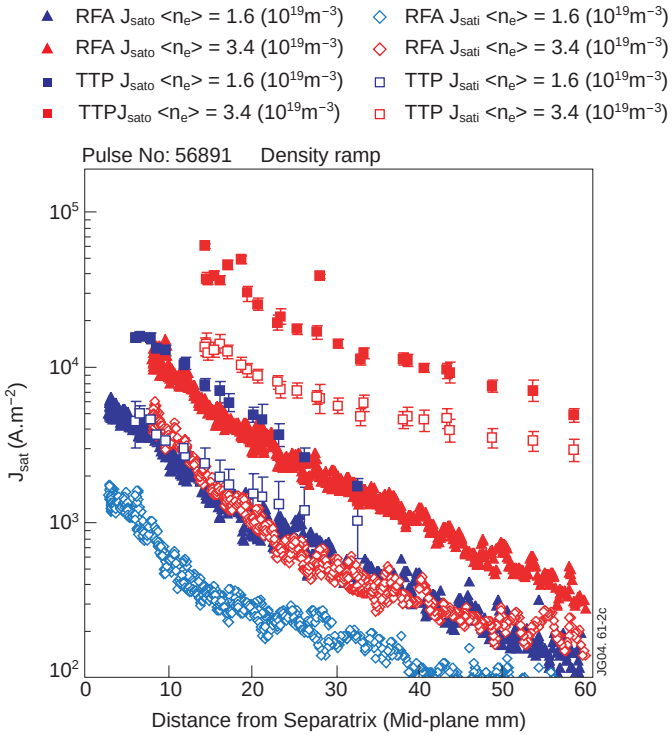

Figure 2: Ion flux densities, j_{sato} and j_{sati}, as measured on each side of the RFA and TTP acting as Mach probes

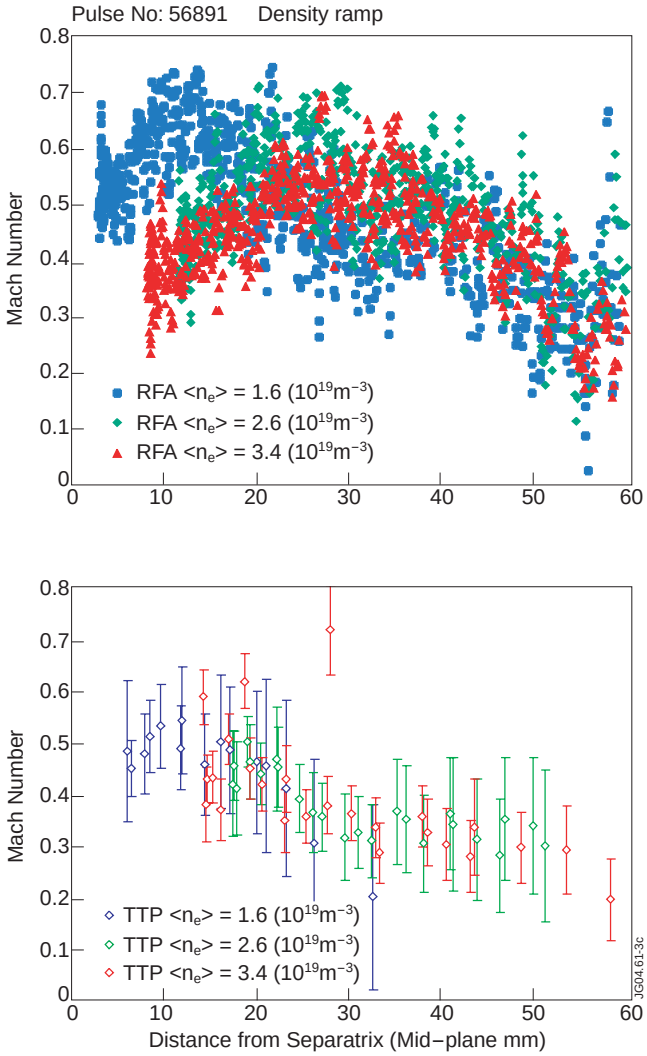

Figure 3. Parallel Flow Mach numbers derived from the data presented in figure 2, for RFA and TTP probe systems, and for 3 different densities during a density ramp.

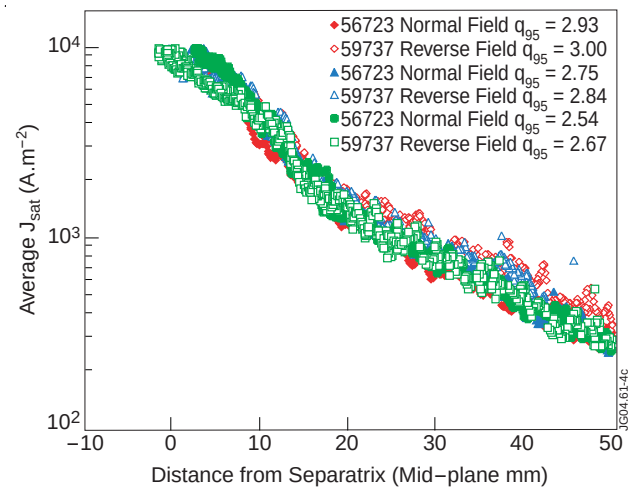

Figure 4: Average flux density profiles in the SOL measured using the RFA in similar discharges with forward and reverse field, for different values of q_{95}.

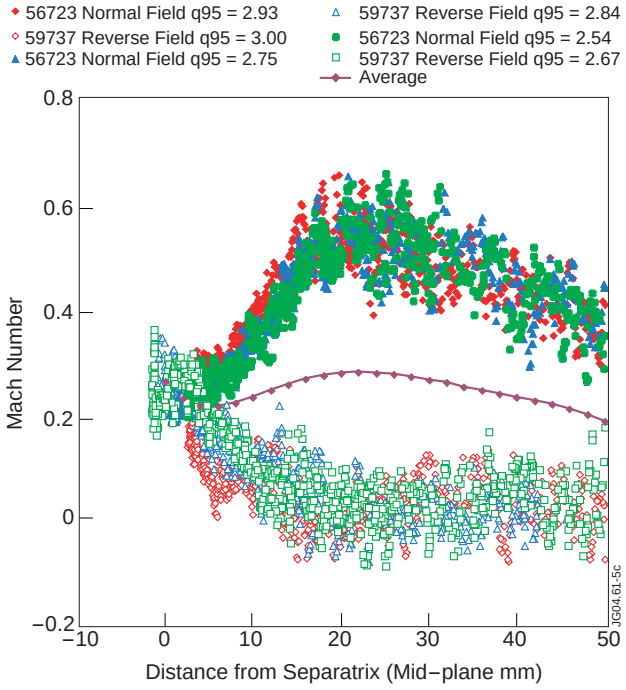

Figure 5: Parallel flow Mach number profiles in the SOL measured using the RFA in similar discharges with forward and reverse field, for different values of q_{95}. The average M(r) from both field directions is also shown.

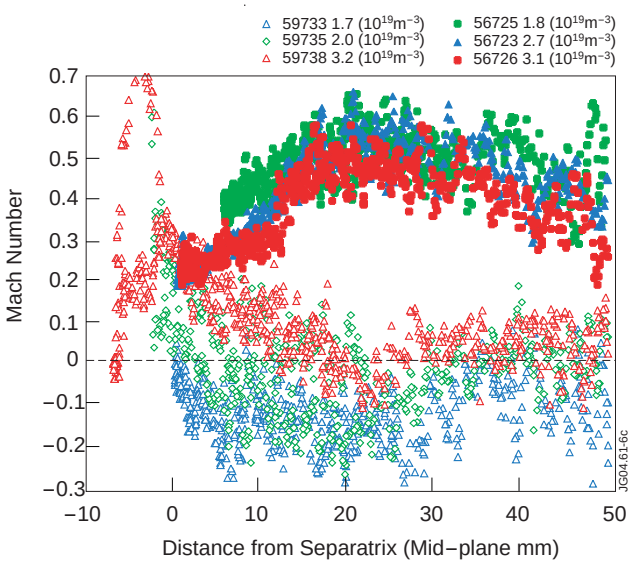

Figure 6: Parallel flow Mach number profiles in the SOL measured using the RFA in discharges with forward and reverse field, for different values of central density $\overline{n}_e$ shown in indent.

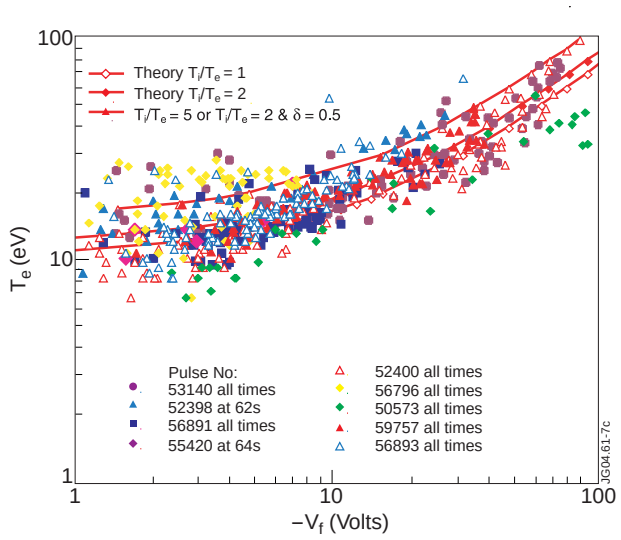

Figure 7: The relationship between T_e and V_f w.r.t target (torus) as measured by the TTP in scanning mode for a large number of JET discharges, ohmic, L and H-mode. Solid line is theory, equation (2), for various T_i/T_e ratios and different see.

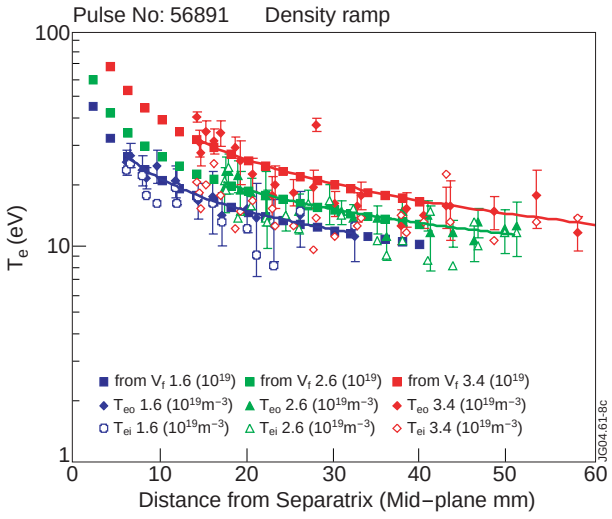

Figure 8: Electron temperatures measured on probes facing outer divertor, T_{eo}, and inner divertor, T_{ei}, of scanning TTP probe, (points with error bars). The squares are from eq.(2) above.

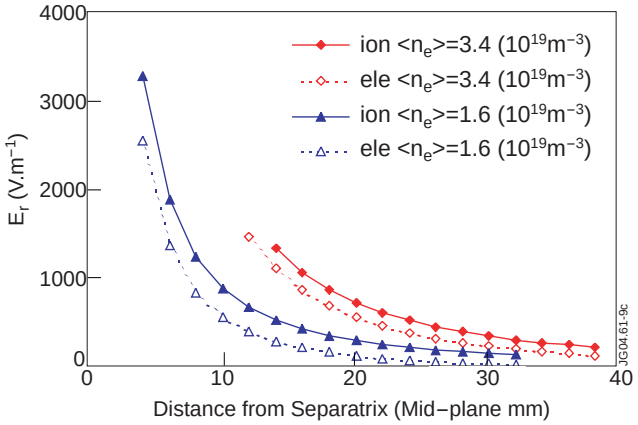

Figure 9: Radial electric field on probes facing outer divertor, Ero, and inner divertor, Eri, of scanning TTP probe, from TTP, deduced from equation 3. Normal field only. The field is the field at the probe, but plotted in mid-plane mm.

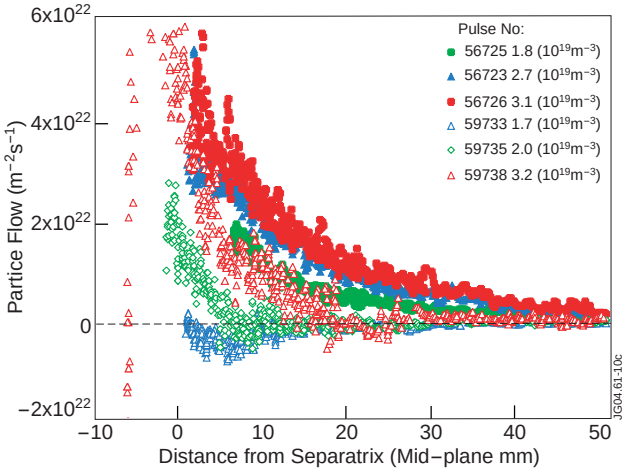

Figure 10: Parallel flow of Particles in the SOL measured using the RFA in discharges with forward and reverse field, for different values of central density $\bar{n}_e$ shown in indent. The solid symbols are for $B \times \nabla B \downarrow$, the open symbols for $B \times \nabla B \uparrow$.

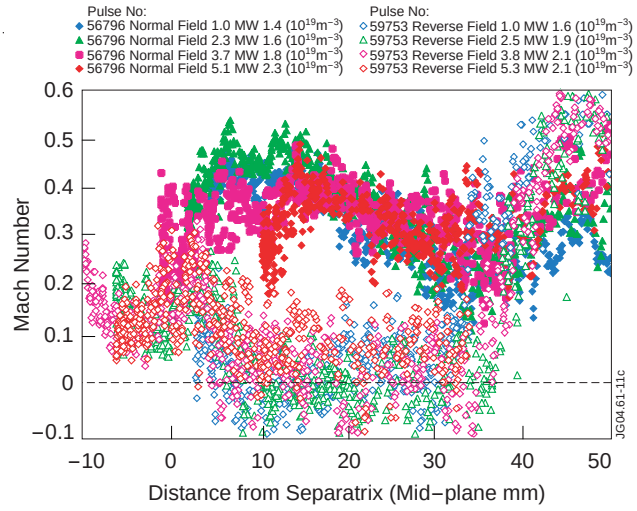

Figure 11: The effect of increasing power on parallel flow Mach number in the SOL. With an increase of neutral beam power, $\bar{n}_e$ also increases as shown.

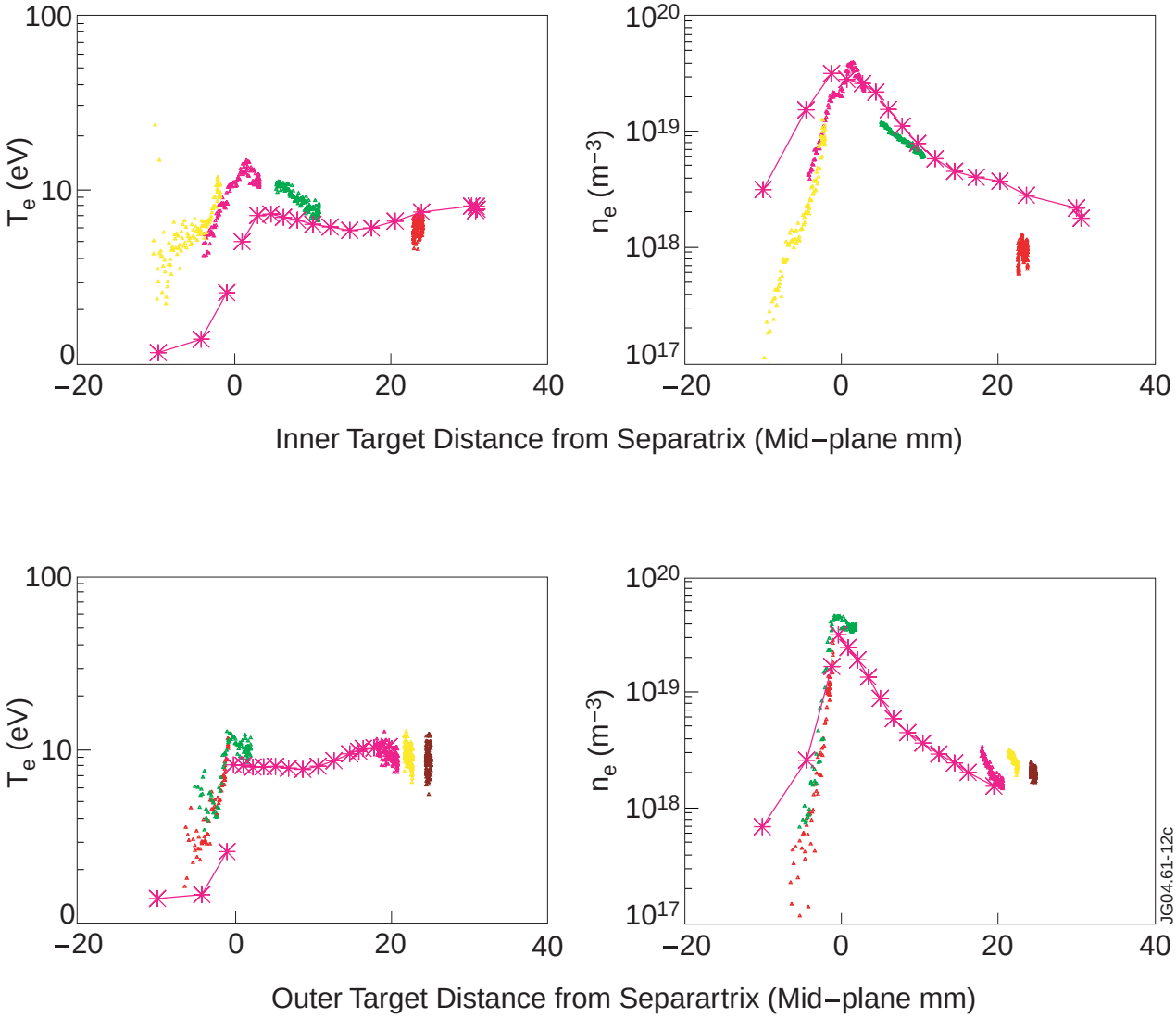

Figure 12: Profiles of density and electron temperature across inner and outer SOL in Reverse field as measured using Target probes, shown as various coloured points from each probe during a small sweep of the separatrix. Also show is the EDGE2D simulation of this case, as red asterisks. Distances < 0 are in the Private region, mapped with the same compression factor as the rest of the SOL to the outside mid-plane. There are no probes available between 5 and 20 mm. This is for the low density case, 59733, $<n_e> = 1.7\ 10^{19}\ m^{-3}$.

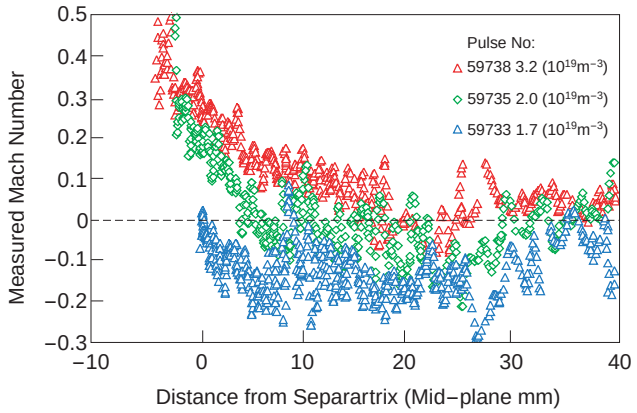

Figure 13a: Measured parallel flow Mach numbers at different values of central density for reverse field discharges.

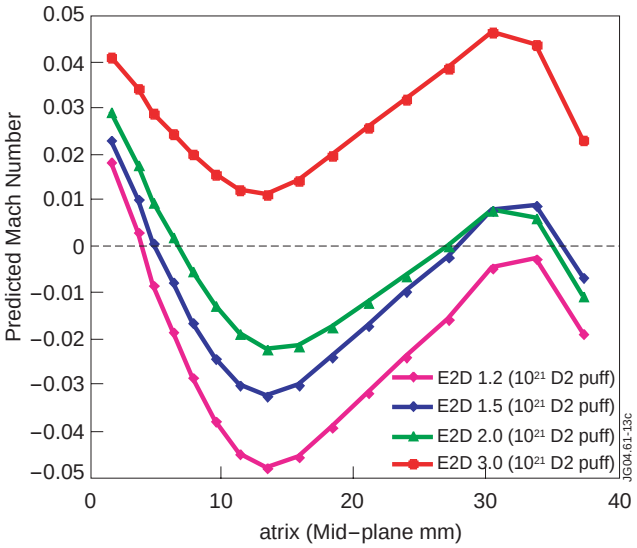

Figure 13b: EDGE2D simulations of the results presented in figure 10a.

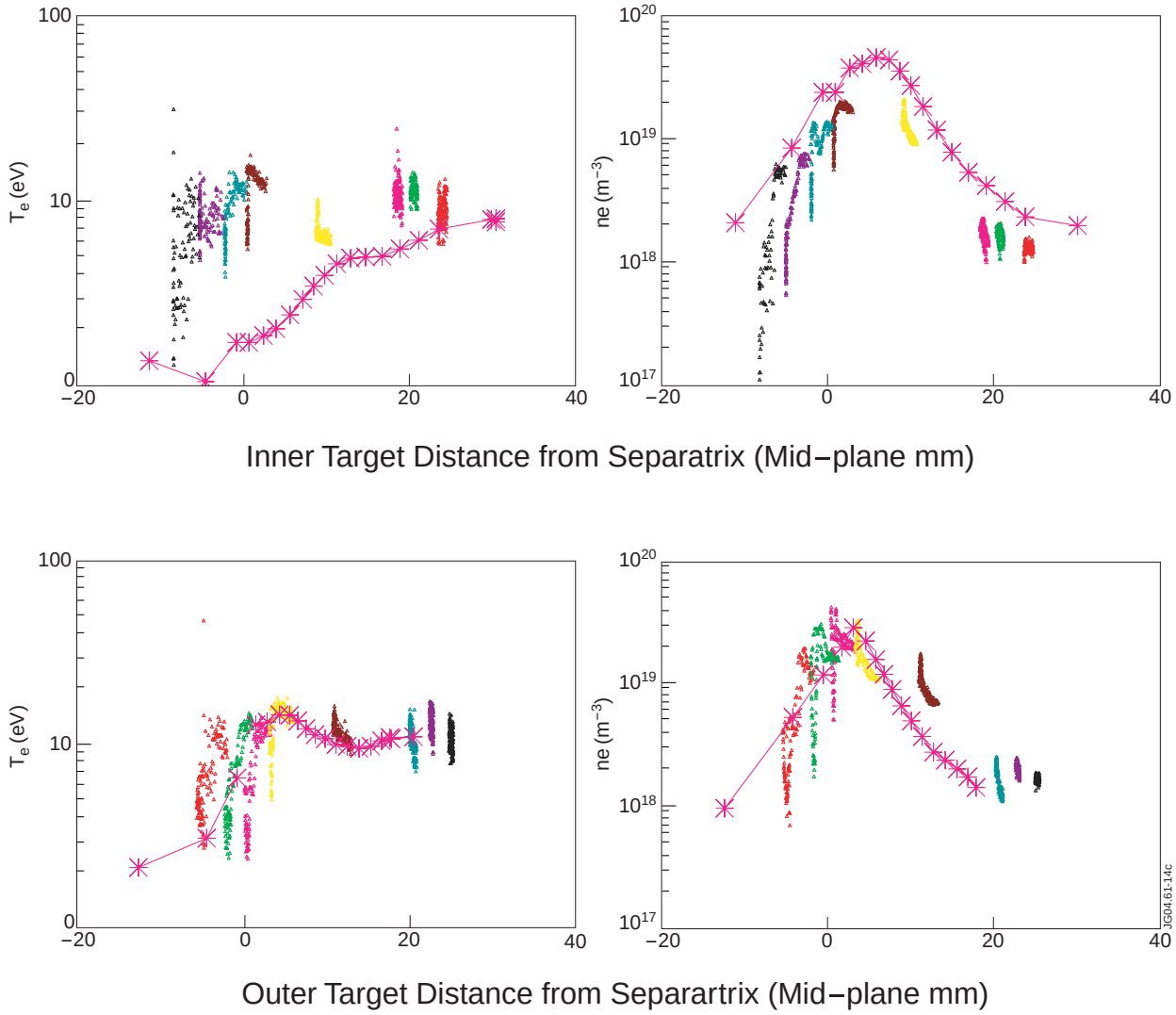

Figure 14: Profiles of density and electron temperature across inner and outer SOL in Forward field as measured using Target probes, shown as various coloured points from each probe during a small sweep of the separatrix. Also show is the EDGE2D simulation of this case, as red asterisks. Distances < 0 are in the Private region, mapped with the same compression factor as the rest of the SOL to the outside mid-plane. This is for the low density case, 56725, $<n_e> = 1.8\ 10^{19}\ m^{-3}$.

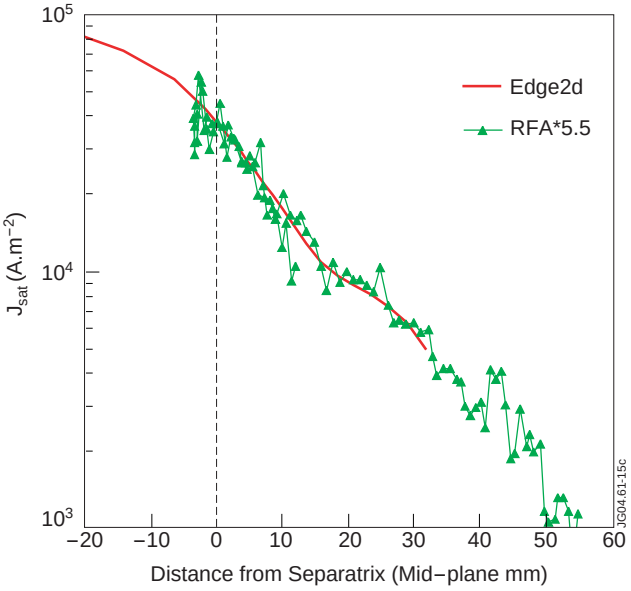

Figure 15: A comparison of the mach number corrected ion saturation current to the RFA (unperturbed flux) with the EDGE2D prediction. The experimental data has to be multiplied by a factor 5.5 to match the code prediction.

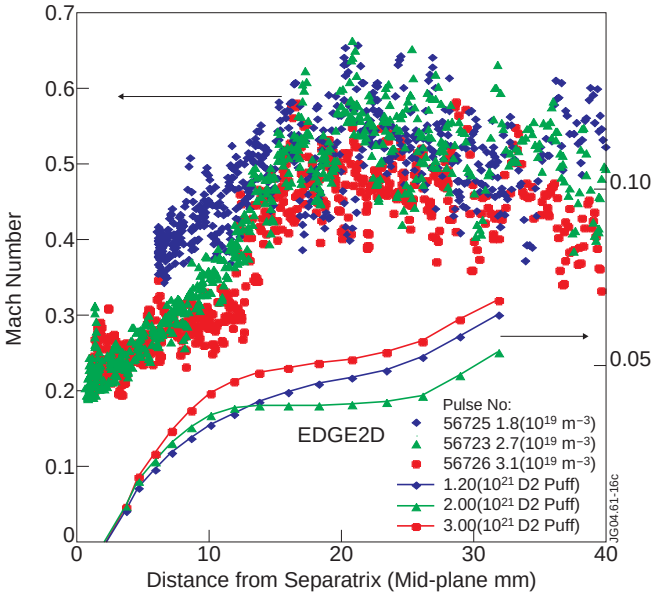

Figure 16: Measured and EDGE2D predicted Mach numbers at different values of central density for reverse field discharges. EDGE2D Mach number predictions for different D_2 puff rates are shown.

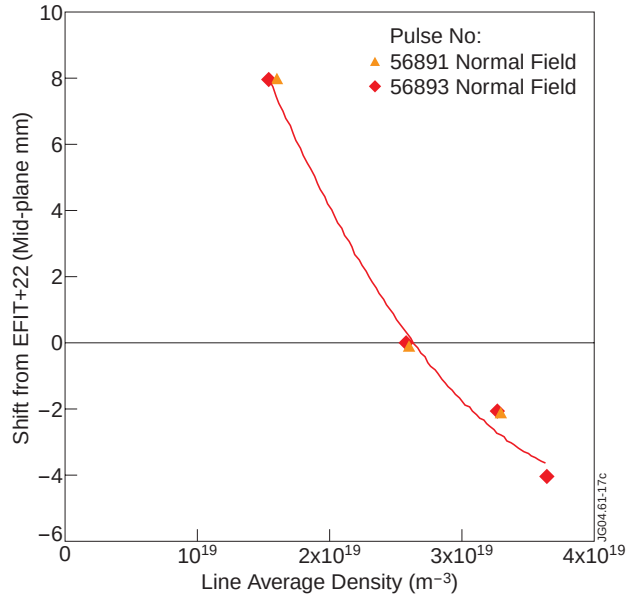

Figure 17: The upstream separatrix position as predicted by EFIT reconstruction compared with that measured assuming electron pressure balance with target probes.

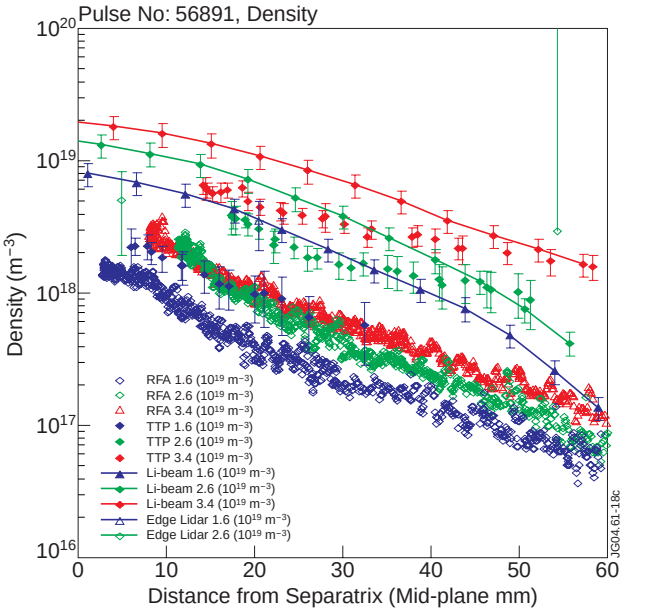

Figure 18: Density profiles as calculated from RFA J_{sato} and TTP T_e compared with those measured by other diagnostics.

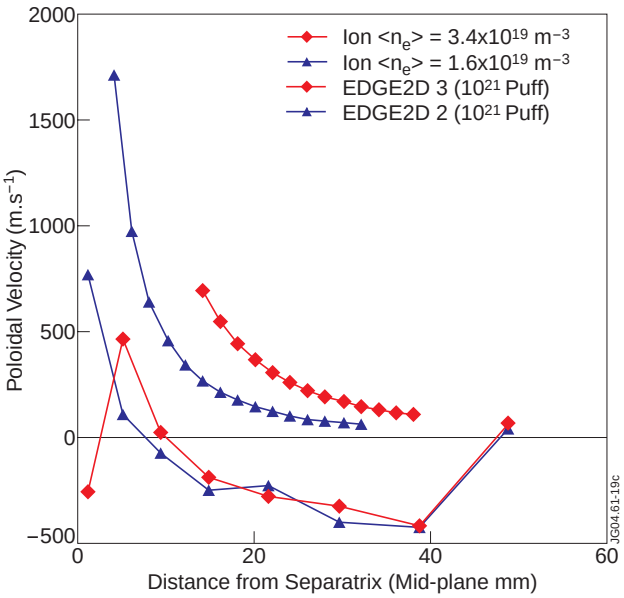

Figure 19: Poloidal flow velocities calculated from experimental measurements, compared with those predicted from the EDGE2D code, at two different densities. Normal field only. Note that these are computed at the probe position, but plotted in mid-plane mm.

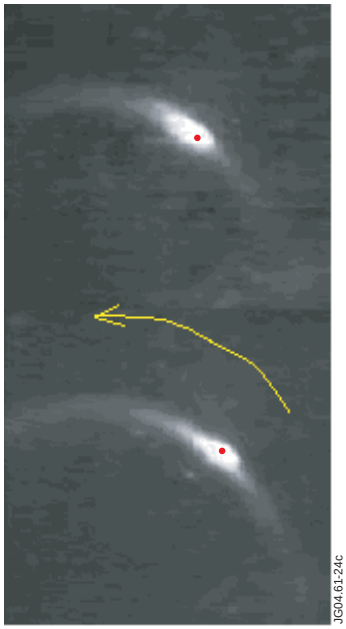

Figure 20: Colour CCD images of the plume from the reciprocating probe. Right to left of the figure is the field line direction outer to inner target. The coloured dot is the probe position.

Top picture: 56723 Forward field.
Bottom picture: 59734 Reverse field.

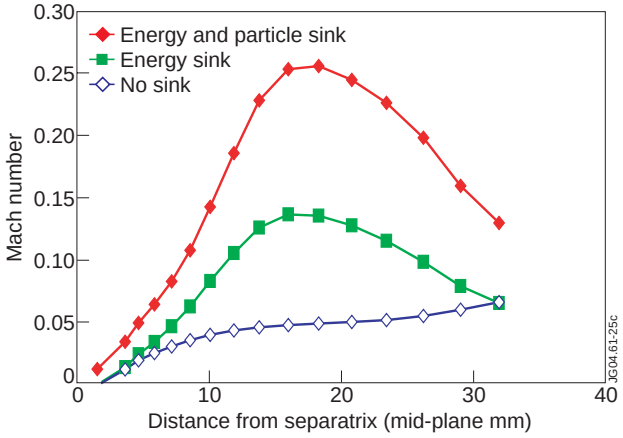

Figure 21: Parallel flow Mach number profiles obtained using EDGE2D for discharge 56723 (see Fig.12), and also for the same discharge with an energy sink just downstream of the probe, and an energy plus particle sink.

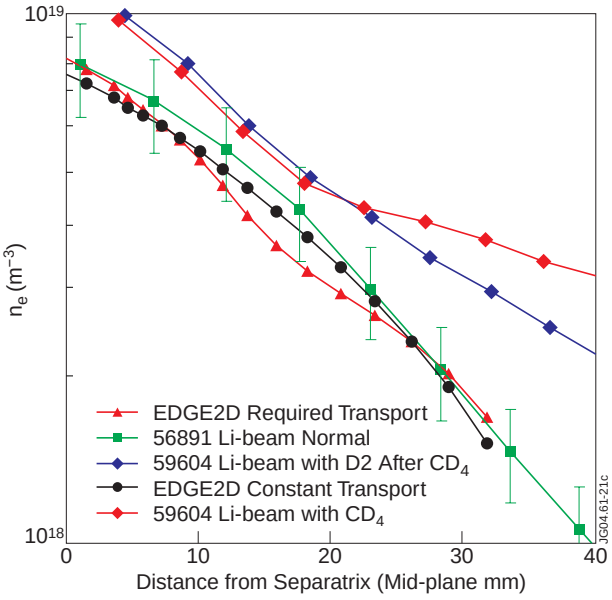

Figure 22: The prediction of upstream density profiles by EDGE2D for $D_\perp(r)$ required to match reciprocating probe density profiles, compared with the $D_\perp(r)$ = 0.5 (i.e. constant) prediction. Lithium beam data is shown for this case, for a result with CD_4 injection, and for just D_2 injection 2s later in the discharge.

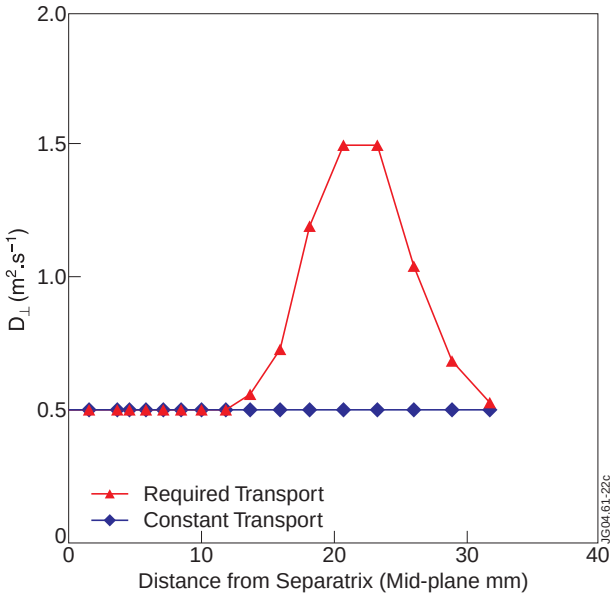

Figure 23: The transport profile, $D_\perp(r)$, required by EDGE2D to reproduce the shape of experimental density profiles as measured by reciprocating probes. The constant transport case, see figure 18, is also shown.